Improvement of slow light performance for vertical-cavity surface-emitting laser using coupled cavity structure*

MA Ya-nan(马雅男)**, **LUO Bin**(罗斌), **PAN Wei**(潘炜), **YAN Lian-shan**(闫连山), **ZOU Xi-hua**(邹喜华), **YI An-lin**(易安林), **YE Jia**(叶佳), and **WEN Kun-hua**(温坤华)

School of Information Science and Technology, Southwest Jiaotong University, Chengdu 610031, China

We propose a vertical cavity semiconductor emitting laser (VCSEL) using a coupled-cavity (CC) design to broaden the bandwidths of gain and delay spectra. The structure is formed by constructing a passive cavity coupled with the active cavity. By rendering the strength of the two resonant cavities, the increased gain bandwidth by 340% and the increased delay bandwidth by 800% are achieved as compared with the signal-cavity (SC) VCSEL. The wideband spectra present more square-like passband which is expected for slow light system. By using it, a 20 Gbit/s super Gaussian signal is delayed by about 13 ps with high quality.

Recently, there have been lots of interests in slow light based on a variety of physical mechanisms, including electromagnetically induced transparency[1,2], stimulated Brillouin scattering[3,4], waveguide dispersion[5] and vertical-cavity surface-emitting lasers (VCSELs)[6,7]. In particular, tunable slow light using VCSEL attracts much attention since it has the advantages of low power consumption, narrow beam divergence and low cost in production[8,9]. Over the last couple of years, many experiments have demonstrated that time delays for sinusoidal signals in VCSELs are dependent on the frequency of modulation[5-10]. However, for pseudo-random binary sequence, which is composed of a series of frequency components, the VCSEL causes serious signal distortion due to its narrow gain and delay bandwidth[11,12]. Therefore, flat gain and delay spectra over all signal bandwidth are highly expected to avoid signal distortion. In this way, it is necessary to find a new method to broaden the bandwidth of the VCSEL in order to satisfy the practical application.

In this paper, we propose a coupled-cavity (CC) structure for VCSELs aimed at providing delay and amplification with desirable broader transmission bandwidths. The model is performed using the Fabry-Perot (F-P) approach and transfer matrix equation. The dependences of the gain and delay spectra on the different CC designs are investigated. An evaluation function is proposed as an easy exploration for optimized design. By utilizing suitable structure, the slow light for 20 Gbit/s super Gaussian pulse can be achieved with very low distortion.

The structure of CC-VCSEL is depicted in Fig.1. It consists of two resonant cavities and three distributed Bragg reflector (DBR) stacks. On the top, the two DBRs are comprised of M_1 and M_2 periods with each thickness of $\lambda_0/2$. These two DBRs and a $\lambda_0/2$-thick low refractive index layer sandwiching between them[13] act as a passive cavity. The passive cavity coupled with the active cavity forms the structure of CC-VCSEL.
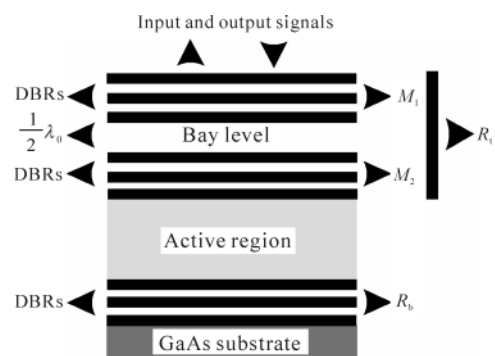

Fig.1 Schematic diagram of CC-VCSEL

In a slow light system, the CC-VCSEL works as an F-P

amplifier giving rise to the group delay due to the coherent population oscillation (CPO) effect[8]. The output signal spectrum is related to the input spectrum through the equation of $\widetilde{E}_{ref}(\lambda) = \widetilde{E}_{in}(\lambda)g(\lambda) \exp[i\psi(\lambda)]$, where $g(\lambda)\exp[i\psi(\lambda)]$ is the transfer function of the device. Utilizing inverse Fourier transform for the output spectrum, the gain of the signal is then obtained by $G(\lambda) = g(\lambda)^2$, and the delay can be derived by $\tau = -d\psi(\lambda)/d\omega$. According to our recent research[12], the formulas of the gain and delay are given in the following:

$$G(\lambda) = \frac{(R_t^{1/2} - R_b^{1/2}G_s)^2 + 4R_t^{1/2}R_b^{1/2}G_s \sin^2\theta}{(1 - R_t^{1/2}R_b^{1/2}G_s)^2 + 4R_b^{1/2}R_t^{1/2}G_s \sin^2\theta} , \quad (1)$$

$$\tau(\lambda) = \frac{2L_c n_c(\sqrt{R_t} - \sqrt{R_t^{-1}})[\sqrt{R_t} + \sqrt{R_t^{-1}} - (\sqrt{R_b}G_s + \sqrt{R_b^{-1}}G_s^{-1})\cos 2\theta]}{c(\sqrt{R_t} - \sqrt{R_t^{-1}})^2 \sin^2 2\theta + [(\sqrt{R_t} + \sqrt{R_t^{-1}})\cos 2\theta - (\sqrt{R_b}G_s + \sqrt{R_b^{-1}}G_s^{-1})]^2} , \quad (2)$$

where R_t and R_b are the reflectivities of the top and bottom mirrors, G_s is the single pass gain, and $\theta = 2\pi n_c L_c(1/\lambda - 1/\lambda_0)$ is the round-trip phase which reflects the detuning between the signal wavelength λ and the cavity resonant wavelength λ_0. For F-P amplifiers, G_s is related to the material gain g_m by the expression of $G_s = \exp(\xi g_m L_a - a_c L_c)$[13], where $\xi=1.75$ is the gain enhancement factor, $L_a = 0.13\ \mu m$ is the total thickness of all quantum wells, $L_c = 2.2\ \mu m$ is the effective cavity length, $a_c = 15\ cm^{-1}$ is the average cavity loss coefficient, and g_m depends on the carrier density by the formula of $g_m(N) = g_0 \ln[(N_s + N)/(N_{tr} + N_s)]$, with the transparency carrier density of $N_{tr}=1.1 \times 10^{18}\ cm^{-3}$[14], and fit parameters of $g_0=1580\ cm^{-1}$ and $N_s=-0.63 \times 10^{18}\ cm^{-3}$.

For our CC structure in Fig.1, the top mirror reflectivity is provided by the designed passive cavity. By treating this cavity as planar thin films, the reflectivity R_t in Eqs.(1) and (2) can be derived by using the transfer matrix equation[15]:

$$\begin{bmatrix} E_{in} \\ E_{ref} \end{bmatrix} = \left\{ \prod_{j=0}^{K} \frac{1}{t_j} \begin{bmatrix} e^{i\delta_j} & r_j e^{i\delta_j} \\ r_j e^{-i\delta_j} & e^{-i\delta_j} \end{bmatrix} \right\} \begin{bmatrix} E_T \\ E_x \end{bmatrix} , \quad (3)$$

where E_{in} is the input signal field, E_T and E_{ref} denote the transmitted and reflected fields, $t_j=2n_{j+1}/(n_j+n_{j+1})$ and $r_j=(n_{j+1}-n_j)/(n_j+n_{j+1})$ are the transmission and reflection coefficients of the interface between the jth and the $(j+1)$th layers, and $\delta_j=(2\pi/\lambda)n_j d_j$ is the complex phase thickness of the jth layer with the refractive index of n_j and the optical thickness of d_j. Under the condition of $E_x = 0$, the passive cavity reflectivity can be calculated by the equation of $R_t = (E_{ref}/E_{in})^2$. Substituting R_t into Eqs.(1) and (2), the gain and delay of CC-VCSEL can be finally obtained.

By using the parameters in Ref.[16], calculations of passive cavity reflectivity for different values of the DBR periods M_1 and M_2 are shown in Fig.2. Since the VCSEL struc-

ture requires high reflectivity to reach reasonable signal gain, M_1 in our design should be far less than M_2. In Fig.2, with increasing M_1 and decreasing M_2, the passive cavity reflectivity at the resonant wavelength drops quickly. This performance is caused by the phase matching for different frequencies. In both cases, the passive cavity working as an F-P cavity provides the signal reflection. The reflectivity becomes lower at the resonant wavelength when the cavity structure tends to be symmetrical[17]. As the signal wavelength is far away from the resonant wavelength, the reflectivity increases because of the enhanced DBR periods.
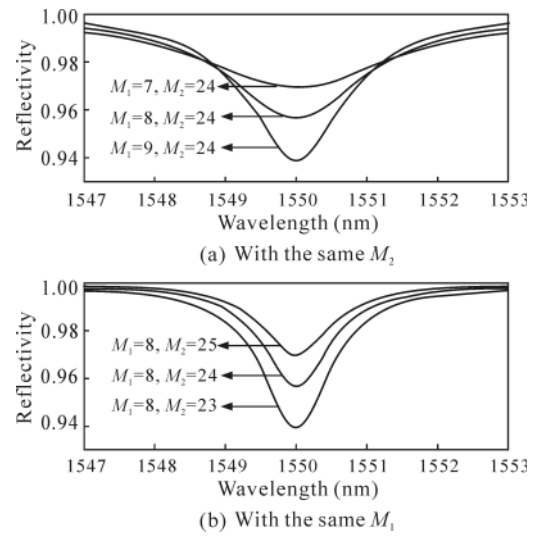

(a) With the same M_2

(b) With the same M_1

Fig.2 Reflectance spectra of passive cavity with different ratios of M_1/M_2

Utilizing the above passive cavity design to construct the CC-VCSEL, Fig.3 shows a comparison of the gain and delay spectra of these structures. When for a fixed M_2, M_1 increases, and for a fixed M_1, M_2 decreases, and the coupled cavity effect becomes more dominant. The peak values of the gain and delay are reduced, and the spectra far from the resonance wavelength are enlarged. The changes easily lead to broader transmission bandwidth, and cause the sharp spectra profile tending to be more square-like and finally forming a valley. The spectrum variation is caused by the designed passive cavity. When the CC-VCSEL is operated in the F-P amplifier mode, the gain value is maximized at resonance wavelength, and declines rapidly, as the wavelength detuning is further increased. However, our design of the passive cavity weakens this effect. The reflectivity reduction at the resonance lowers the peak gain. Then, the increased reflectivity with the enlarged wavelength detuning enhances both sides of the gain profile. Considering the Kramas-Kronig (K-K) relation[6], this gain variation depends on corresponding delay spectrum changes. Thus, the wideband gain and delay spectra can be obtained by using the CC design.
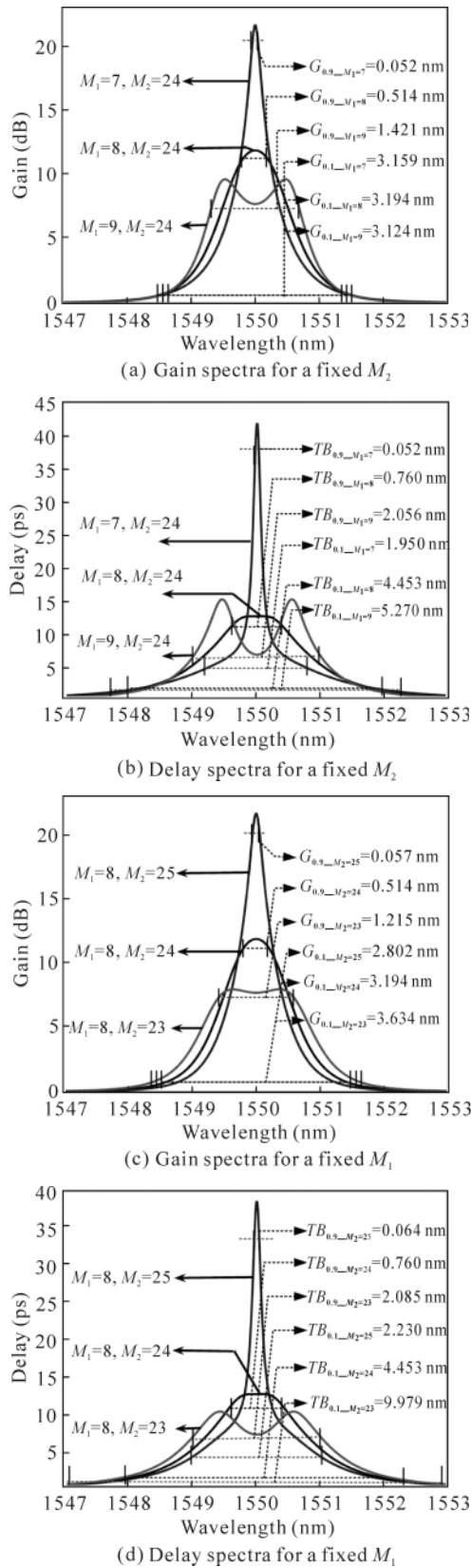
(a) Gain spectra for a fixed M_2

(b) Delay spectra for a fixed M_2

(c) Gain spectra for a fixed M_1

(d) Delay spectra for a fixed M_1

Fig.3 Gain and delay spectra of CC-VCSELs with different ratios of M_1/M_2

In order to compare the performance of the above CC-VCSEL structures in slow light system, Tab.1 shows the char-

acteristic parameters of their transfer functions, where $\varepsilon_{G(T)}= G_{0.9}(TB_{0.9})/G_{0.1}(TB_{0.1})$ is the rectangle factor, which represents the quotient of the full bandwidth of 90% peak values divided by 10% values in gain and delay spectra, and $\xi_{G(T)}= [G_{max}(T_{max})-G_{min}(T_{min})]/G_0(T_0)$ is the ripple coefficient, which means the ratio of the maximum and minimum difference in 90%−100% peak range with the value of $G_0(T_0)$ at the resonance wavelength. In Tab.1, our calculations indicate that wider bandwidth and better rectangle factor for the transmission spectra profile can be achieved at the cost of lower gain and delay values and larger ripple coefficient. Thus, in order to obtain a preferable trade-off, we propose an evaluation function as follows:

$$\varphi = W_1\varepsilon_G^2 + W_2(1-\xi_G)^2 + W_3\varepsilon_T^2 + W_4(1-\xi_T)^2 , \tag{4}$$

where $W_1 \cdots W_4$ are the weight factors, which are evaluated by 0.25 in Tab.1. The calculations of φ in Tab.1 show the design of $M_1 = 8$ and $M_2 = 24$ could render the strength of the coupled cavity comparably. By using this structure, Fig.4 shows the comparison of the gain and delay spectra of the CC-VCSEL and the SC-VCSEL. The corresponding characteristic parameters of the two structures are shown in Tab.2. These calculations are performed for a fixed peak gain of 12 dB and a group delay of 13 ps. The results reflect that by using the CC structure, the gain bandwidth about 64.1 GHz is

Tab.1 Characteristic parameters of five different CC-VCSEL structures

Structure	G_0 (dB)	$G_{0.9}$ (GHz)	ε_G (%)	ξ_G (%)	T_0 (ps)	$TB_{0.9}$ (GHz)	ε_T (%)	ξ_T (%)	φ (%)
$M_1=7,M_2=24$	21.8	6.5	1.6	2.3	42.0	6.5	2.7	10.0	44.6
$M_1=8,M_2=24$	11.9	64.1	16.1	4.2	12.9	95.0	17.1	10.0	48.4
$M_1=9,M_2=24$	7.7	177.6	39.0	31.4	7.0	257.0	39.0	29.8	25.25
$M_1=8,M_2=23$	7.7	151.9	33.4	9.8	7.4	260.6	20.9	52.1	29.8
$M_1=8,M_2=25$	21.7	7.1	2.0	2.3	38.7	8.0	2.9	10.0	45.1

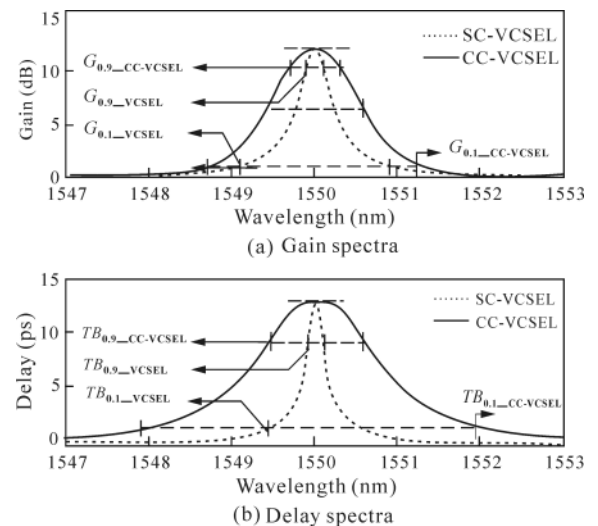(a) Gain spectra

(b) Delay spectra

Fig.4 Gain and delay spectra of CC-VCSEL and SC-VCSEL

obtained, which is 340% broader than that of the SC-VCSEL. Meanwhile, the rectangle factor is increased by 160% for the gain spectrum. Similarly, the CC structure also provides 95 GHz delay bandwidth, which is 800% larger than that of the SC structure, and the corresponding rectangle factor is increased by 240% than its reference.

Tab.2 Characteristic parameters of CC-VCSEL and SC-VCSEL

Component	$G_{0.9}$ (GHz)	ε_G (%)	ξ_G (%)	$TB_{0.9}$ (GHz)	ε_T (%)	ξ_T (%)
CC-VCSEL	64.1	16.1	4.2	95.0	17.1	10.0
SC-VCSEL	18.7	10.3	4.2	11.9	7.2	10.0

Utilizing the above two devices into the slow light system, Fig.5 shows the time-domain delay traces of the 20 Gbit/s super Gaussian pulses in CC-VCSEL and SC-VCSEL, respectively. The result indicates that a better signal quality can be obtained by using the CC structure. The dominant contribution for the low signal distortion comes from the broader gain and delay bandwidth. More importantly, the square-like shape with steeper sides ensures the flat gain and delay spectra over all signal bandwidths. These advantages of CC design indicate a very desirable characteristic for slow light system, and promise the CC-VCSELs to meet the practical need in the future.
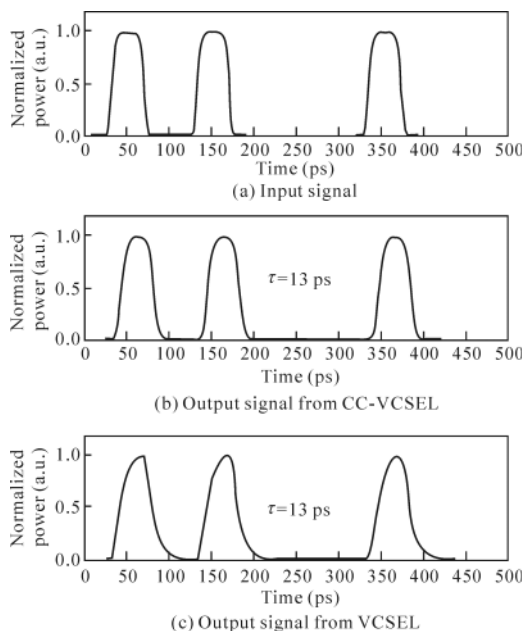

Fig.5 Slow light of 20 Gbit/s super Gaussian signals in CC-VCSEL and SC-VCSEL

In conclusion, we present a CC structure to broaden the gain and delay bandwidth for VCSELs. By using the evaluation function to choose desirable structure, a highly increased gain bandwidth as much as 340% is calculated, and a very large delay bandwidth about 95 GHz can be obtained with more square-like passband shape. Utilizing this design in slow light system, it makes the 20 Gbit/s super Gaussian pulse delayed by about 13 ps without any distortion.

References

[1]   L. V. Hau, S. E. Harris, Z. Dutton and C. H. Behroozi, Nature **397**, 594 (1999).

[2]   J. C. Liang, H. H. Wang and Z. K. Jiang, Acta Optica Sinica **27**, 946 (2007). (in Chinese)

[3]   Z. Zhu, A. M. C. Dawes, D. J. Gauthier, L. Zhang and A. E. Willner, J. Lightwave Technol. **25**, 201 (2007).

[4]   YIN Jing-chan, XIAO Xiao-sheng and YANG Chang-xi, Journal of Optoelectronics • Laser **21**, 786 (2010). (in Chinese)

[5]   Y. D. Zhang, W. Weng, B. Yu and P. Yuan, Laser and Optoelectronics Progress **44**, 26 (2007). (in Chinese)

[6]   X. Zhao, P. Palinginis, B. Pesala, C. H. Connie and H. Philip, Opt. Express **13**, 7899 (2005).

[7]   SHI Jing-jing, TIAN Zhen-hua, QIN Li, ZHANG Yan, WANG Zhen-fu, LIANG Xue-mei, YANG Ye, NING Yong-qiang, LIU Yun and WANG Li-jun, Journal of Optoelectronics • Laser **21**, 1445 (2010). (in Chinese)

[8]   P. C. Peng, F. M. Wu, C. T. Lin, J. Chen, P. T. Shih, W. C. Kao, W. J. Jiang, H. C. Kuo and S. Chi, Tunable Slow Light in Quantum Well Vertical-Cavity Surface-Emitting Laser at 40 GHz, Quantum Electronics and Laser Science Conference **JThA**, JThA2 (2008).

[9]   C. H. Connie, P. C. Ku, J. Kim and S. L. Chuang, Proceedings of the IEEE **91**, 1884 (2003).

[10] P. C. Peng, C. T. Lin, H. C. Kuo, J. N. Liu, W. K. Tsai, G. Lin, H. P. Yang, K. F. Lin, J. Y. Chi and S. C. Wang, Tunable Slow Light using Quantum Dot VCSEL for Subcarrier Multiplexed System, Optical Fiber Communication Conference **OThT**, OThT6 (2007).

[11] Y. N. Ma, B. Luo, W. Pan, L. S. Yan, X. H. Zou, A. L. Yi, J. Ye, K. H. Wen and D. Zheng, Acta Phys. Sin. **61**, 14215 (2012). (in Chinese)

[12] Y. N. Ma, B. Luo, L. S. Yan, W. Pan, X. H. Zou, J. Ye, A. L. Yi and D. Zheng, Chin. Opt. Lett. **9**, 51401 (2011).

[13] S. F. Lim and C. H. Connie, IEEE Photon. Technolo. Lett. **7**, 1240 (1995).

[14] J. H. Xu, B. Luo, W. Pan, Z. N. Qin and F. Wang, Opto-Electronic Engineering **34**, 100 (2007). (in Chinese)

[15] G. Wang, B. Luo, W. Pan and J. Xiong, Chin. Phys. Lett. **22**, 2561 (2005).

[16] E. S. Bjorlin, B. Riou, P. Abraham, J. Piprek, Y. Y. Chiu, K. A. Black, A. Keating and J. E. Bowers, IEEE J. Quantum Electron. **37**, 274 (2001).

[17] C. Z. Guo and S. L. Chen, Acta Phys. Sin. **46**, 1731 (1997). (in Chinese)